Sulfur speciation in *Sphagnum* peat moss modified by mutualistic interactions with cyanobacteria

Elizabeth Herndon[1] (0000-0002-9194-5493), Jocelyn Richardson[2] (0000-0002-0671-9265), Alyssa A. Carrell[3] (0000-0003-1142-4709), Eric Pierce[1] (0000-0002-4951-1931), David Weston[3] (0000-0002-4794-9913)

[1]Environmental Sciences Division, Oak Ridge National Laboratory, Oak Ridge, TN, 37830, United States
[2]SLAC National Accelerator Laboratory, Menlo Park, CA, 94025, United States
[3]Biological Sciences Division, Oak Ridge National Laboratory, Oak Ridge, TN, 37830, United States

Corresponding author: Elizabeth Herndon (herndonem@ornl.gov)

Introduction: 1206 words
Materials and Methods: 1067 words
Results: 830 words
Discussion: 998 words (24% of text)
Number of figures: 8 (all should be published in color)
Tables: Tables 1 and 2
Supporting information: Figures S1, S2, and S3

Summary

- Peat moss (*Sphagnum spp.*) develops mutualistic interactions with cyanobacteria by providing carbohydrates and S compounds in exchange for N-rich compounds, potentially facilitating N inputs into peatlands. Here, we evaluate how colonization of *Sphagnum angustifolium* hyaline cells by *Nostoc muscorum* modifies S abundance and speciation at the scales of individual cells and across whole leaves.
- For the first time, S K-edge X-ray Absorption Spectroscopy was used to identify bulk and micron-scale S speciation across isolated cyanobacteria colonies, and in colonized and uncolonized leaves.
- Uncolonized leaves contained primarily reduced organic S and oxidized sulfonate- and sulfate-containing compounds. Increasing *Nostoc* colonization resulted in an enrichment of S and changes in speciation, with increases in sulfate relative to reduced S and sulfonate. At the scale of individual hyaline cells, colonized cells exhibited localized enrichment of reduced S surrounded by diffuse sulfonate, similar to observations of cyanobacteria colonies cultured in the absence of leaves.
- We infer that colonization stimulates plant S uptake and the production of sulfate-containing metabolites that are concentrated in stem tissues. Sulfate compounds that are produced in response to colonization become depleted in colonized cells where they may be converted into reduced S metabolites by cyanobacteria.

Plain Language Summary: Peat moss is a plant that forms a beneficial relationship with cyanobacteria in order to obtain nitrogen, a key nutrient. We show that peat moss contains more of a different nutrient, sulfur, when it interacts with cyanobacteria, presumably for the purpose of exchanging sulfur for nitrogen.

Keywords: sulfur, S*phagnum*, cyanobacteria, x-ray microprobe, x-ray absorption spectroscopy, peat moss

Introduction

Sphagnum peat mosses are key members of peatland ecosystems that comprise one of the largest global carbon (C) sinks. Plant production in peatlands outpaces decomposition due to the unique chemical and functional characteristics of peat mosses together with typically cold, acidic and anoxic environmental conditions (Clymo & Hayward, 1982). Over millennial timescales, the production to decomposition mismatch has resulted in the accumulation of *c*. 30% of all soil C in just 3% of the global land surface (Yu, 2012), creating a critical atmospheric C sink that is highly sensitive to climate variability (Yu et al., 2003; Belyea and Malmer, 2008). Warming and drought events associated with ongoing climate change are hypothesized to decrease production while increasing decomposition, resulting in the transition of C sink to C source (Dorrepaal et al. 2009). Recent results from a whole peatland warming and CO_2 manipulation study support this hypothesis by finding that warming resulted in *Sphagnum* mortality (Norby et al. 2019) and an increase in shrub density that correlated with an atmospheric C sink to source transition resulting from increased CO_2 and CH_4 emissions (Wilson 2016, Hanson et al. 2020).

Much of the ecological success of *Sphagnum* peat mosses are attributed to its symbiotic interactions with associated microorganisms; for example, N_2-fixing symbionts can provide a large proportion (20-30%) of *Sphagnum*'s nitrogen (Kostka et al. 2016, Weston et al. 2015). Early studies discovered that N_2-fixing cyanobacteria reside on cell surfaces and within water-filled hyaline cells of *Sphagnum* (Basilier et al. 1978, Basilier 1979, Granhall and Hafsten 1976). More recent studies have shown that *Sphagnum* associates with a diverse assemblage of microorganisms that help mediate host tolerance to warming (Carrell et al. 2022), N_2-fixation, and methane oxidation (Kip et al. 2010) processes that can scale to impact ecosystem C and N cycling (Lindo et al. 2013, Carrell et al. 2022, Petro et al., 2023). Current understanding of the *Sphagnum* - cyanobacterium symbiosis is that C-rich carbohydrates are exchanged for N-rich molecules, but this conceptual model appears to be overly simplistic and possibly missing a key role for sulfur (S). In a study by Warshan et al. (2017), comparative genomics was used to investigate gene family relationships among N_2-fixing cyanobacteria that are symbiotically competent and non-competent with feathermosses (*Pleurozium schreberi*). The investigators identified 32 gene families that were specific to symbiotically competent genomes involved in chemotaxis and motility, NO regulation, and glycosyl-modifying and oxidative stress-mediating exoenzymes. In addition, the investigators found genes involved in sulfate transport. This unexpected finding led Stuart et al. (2020) to pair isotope probing with high-resolution imaging mass spectrometry (NanoSIMS) to demonstrate that both C and S are transferred from the *P. schreberi* moss host to cyanobacteria in exchange for N. To further demonstrate a role for S, the investigators knocked out the cyanobacteria sulfonate monoxygenase gene that catalyzes the conversion of alkane sulfonates to sulfite (van der Ploeg et al. 2001). The loss of a functional sulfonate monoxygenase

resulted in the inability of cyanobacteria to colonize *P. schreberi*, further suggesting a role for S transfer from plants to cyanobacteria in promoting symbiosis and resulting N_2-fixation.

While the understanding of S impact on N_2-fixation in moss systems is currently limited, the body of research concerning Rhizobium-legume symbiosis is much more extensive. For example, S deficiency has long been shown to reduce N_2-fixation rates (e.g., Janssen & Vitosh, 1974, Shock et al. 1984). Conversely, S addition has consistently been shown to enhance N_2 fixation. These patterns have been observed across various legumes, including kidney beans (*Phaseolus vulgaris L.*; Janssen & Vitosh, 1974), subclover (*Trifolium subterraneum*; Shock et al., 1984), field peas (*Pisum sativum L.*; Sherer et al., 2006), and red clover (*Trifolium pratense*; Scherer and Lange, 1996). Nonetheless, the precise mechanisms through which S influences N_2-fixation have yet to be fully elucidated. Sulfur deficiency might impede protein synthesis, leading to an accumulation of protein precursors such as amino acids. This accumulation, in turn, could exert a negative feedback effect on N_2-fixation (Varin et al., 2009). Moreover, substantial quantities of S are necessary to facilitate the formation of Fe–S clusters, which are integral components of the nitrogenase active site. These studies underpin the potentially critical role of S in facilitating symbiosis between plants and N_2-fixing bacteria more broadly.

Sulfur inputs to *Sphagnum*-dominated, ombrotrophic peatlands derive largely from sulfate deposition in dust and meteoric precipitation (Urban et al., 1989), although contributions from the latter have decreased in impacted areas in recent decades due to decreased industrial S emissions. Sulfate is typically an abundant resource, and plants can acquire approximately half of their S directly from deposited sulfate with much of the remainder coming from peat mineralization, i.e., microbial conversion of organic S compounds contained in peat to inorganic sulfate (Urban et al., 1989). Sulfate also serves as a terminal electron acceptor for anaerobic sulfate reduction, which is a dominant metabolism in freshwater peatlands (Vile et al., 2003; Lin et al., 2014). Reduced S compounds produced through sulfate reduction are incorporated into microbial and plant biomass, and subsequently retained in saturated, anoxic peat at depth (Urban et al., 1989). While S is generally available in excess of nutritional requirements, peatlands are often N-limited. Nitrogen inputs to many ombrotrophic peatlands derive largely from atmospheric deposition of nitrate and ammonium (Limpens et al., 2006; Urban and Eisenreich, 1988). However, biological N_2-fixation often exceeds N deposition in northern peatlands and can alleviate N limitation (Limpens et al., 2006; Urban and Eisenreich, 1988; Lin et al., 2014; Yin et al., 2022). Indeed, *Sphagnum* can obtain a large portion of its N from N_2-fixing symbionts (Kostka et al., 2016; Weston et al., 2015), indicating an important role for moss-cyanobacteria symbiosis in supporting peatland ecosystems.

To further investigate the metabolism of moss - cyanobacteria symbiosis, co-transcriptome (Carrell et al. 2020), spatial metabolic profiling (Veličković et al 2018, Nagy et al. 2019), and metabolic cross-feeding

(Carrell et al. 2022) studies were conducted with *Sphagnum angustifolium*. Results indicated that S-rich compounds choline-O-sulfate and taurine were produced by the moss host and depleted by the cyanobacteria. Choline-O-sulfate can serve as a compatible solute to alleviate osmotic stress in bacteria and plants (MacKay et al. 1984, Reed et al. 1984, Csonkia 1989), leading Carrell et al. (2022) to conclude that the *Sphagnum*-cyanobacterium symbiosis goes beyond the traditional view of C and N exchange and includes S-containing metabolites for nitrogenase synthesis and survival in harsh anoxic and low pH conditions common to peatlands.

Previous studies measured metabolite exchange between *Sphagnum* and cyanobacteria that were physically separated (Carrell et al., 2022, Nagy et al. 2019, Veličković et al 2018). However, metabolite exchange within colonized leaves and the effects of colonization on whole plant S dynamics remain unexplored. In this study, our objective was to evaluate the effect of colonization on the abundance and distribution of S species within intact *Sphagnum* leaves. We used micro-X-ray Fluorescence (μXRF) mapping coupled with S K-edge X-ray Absorption Near Edge Structure (XANES) spectroscopy to investigate the average S speciation in *Sphagnum* tissues as well as the spatial distributions of S species in isolated cyanobacteria colonies and in intact leaves and stems that were either uncolonized or colonized by cyanobacteria. Although these techniques cannot identify individual metabolites, they provide micron-scale resolution of the relative proportions of major S functional groups.

Materials and Methods

Sample preparation

Nostoc muscorum UTEX 1037 was cultivated in a 250 mL flask with a final volume of 100 mL at 24 °C in BG-11_0 medium at pH 8.2 and shaken at 125 rpm with a 16 h/8 h (day/night) cycle at 150 photosynthetically active radiation (PAR) for 21 days. Axenic *Sphagnum angustifolium* cultures from Oak Ridge National Laboratory (ORNL) were maintained on Knop's medium at pH 5.7 with a 16 h/8 h (day/night) cycle at 150 PAR. The Knop's medium contained much lower S and N than present in other growth media *(*1.84 mM potassium dihydrogen phosphate, 3.35 mM potassium chloride, 1.01 mM magnesium sulphate, 4.24 mM calcium nitrate, 45 μM iron(II) sulphate*).* For colonization, an aliquot of *Nostoc muscorum* UTEX 1037 was pelleted through centrifugation, media removed, and then resuspended in fresh BG11 -N media. A total of 2 mL of *Nostoc* culture (100 mg mL^{-1} BG-11_0 medium at pH 5.0) was added to a well of a 12 well plate. *S. angustifolium* tissue culture plants originated from field collected material that was surface sterilized and propagated asexually (Carrell et al., 2022). *S. angustifolium* gametophytes (~10 mg dry weight [DW]) were placed in a fitting cell culture insert (8 μm membrane pore size). Each insert was placed in the *Nostoc* filled

well for colonization. *S. angustifolium* cultures without *Nostoc* present below the cell inserts were used as negative controls.

After 14 days, leaf colonization was examined under an epifluorescence microscope equipped with a green (510–560 nm) and red excitation filter. Green and red in the epifluorescence image were later converted to gold and pink, respectively, for visualization. Leaves were harvested from across the branch. The inoculated *Sphagnum* samples contained both epiphytic and endophytically colonized leaves; however, to enable localization of S distribution, only leaves with full endophytic colonization were targeted for spectroscopic analysis. Colonization (%) was quantified as the percent of *Sphagnum* hyaline cells occupied by *Nostoc* compared to non-occupied hyaline cells for a given leaf. Whole leaves were defined as colonized if percent colonization was >1% (n = 11) and uncolonized if percent colonization was < 0.01% (n = 7). Uncolonized leaves included leaves from four negative control samples that were uninoculated as well as three inoculated samples with < 0.01% colonization. Individual leaves or clusters of leaves were removed with sterile forceps, gently rinsed in deionized water to remove excess media, and placed flat on a glass microscope slide, covered with S-free tape (St. Gobain), and shipped to the Stanford Synchrotron Radiation Lightsource (SSRL) for XRF and XANES spectroscopy. Isolated *Nostoc* cultures were also pipetted onto a glass slide, covered with S-free tape, and examined with XRF and XANES.

Synchrotron XRF imaging and XANES spectroscopy

Sulfur K-edge μ-XRF imaging and XANES spectroscopy were performed at SSRL beamline 14-3, SLAC National Accelerator Laboratory. X-ray measurements were performed under standard SPEAR3 ring conditions of 500 mA and 3 GeV. The double Si (111) crystal monochromator at BL14-3 was calibrated to the S K-edge using the first pre-edge peak of powdered sodium thiosulfate (2472.02 eV). An x-ray beam of 1x1 mm was selected using slits for bulk XANES spectroscopy. The bulk beam was further focused to 1 or 5 micrometers immediately before the sample using Sigray paraboloidal lenses. A N_2-purged 7-element Hitachi Vortex Si-drift detector was used in fluorescence mode for all measurements. Samples were mounted onto a 360° rotating stage in a He-purged chamber at room temperature for analyses.

Bulk XANES spectra were obtained on leaf clusters that included branches and stems, with 3-6 repeat XANES spectra per cluster depending on the quality of spectra. Spectra were averaged to improve signal to noise (using SIXpack; Webb (2005)) and normalized by regressing a line function to the pre-edge and by fitting a linear polynomial to the post-edge region. Linear combination fitting (LCF) of standard XANES spectra (elemental sulfur, l-cysteine, l-methionine, dibenzyl sulfide, DL methionine sulfoxide, sodium cyclohexanesulfonate and sodium sulfate; Manceau and Nagy (2012)) to experimental data was performed

in Larch (Newville, 2013). Standard spectra were aligned to our experimental data by aligning Na cyclohexanesulfonate in the reference database to the peak of maximum intensity in our Na thiosulfate calibration as they are both SO_3 bearing (a shift of -0.23 eV was applied to all reference spectra). Results are reported as the relative proportion of S functional groups represented by the standard spectra, including elemental S (S^0), reduced organic S (R-S-H and R-S-S-R'), sulfoxide (R-S(O)-R'), sulfonate (R-SO_3-H), and sulfate (R-SO_4-H) (Prietzel et al., 2018; Pierce et al., 2022). Reduced organic S encompasses l-cysteine, l-methionine, and dibenzyl sulfide, which are spectroscopically similar, although methionine was the primary contributor to the best fits.

Leaves for XRF mapping were chosen based on % colonization. Maps of leaves were obtained using a 1 micron beam spot size, a 3 micron step size and 80 ms dwell time. Maps were collected at multiple energies (ME) of 2470.8, 2473.05, 2473.4, 2478.0, 2481.0 and 2482.1 eV based on preliminary XANES spectra and reported literature values of S species anticipated to be present in these samples. Spot locations for micro-XANES spectroscopy were determined using a principal component analysis of the raw ME maps. Additional spot XANES locations were chosen based on differences in fluorescence in raw maps. Micro-XANES spectra were processed as reported above for bulk spectra. XRF maps were processed in the Microanalysis Toolkit (Webb, 2006) by first applying a gaussian smoothing function to an area of 5x5 pixels (standard deviation of 0.8) to each ME map. A non-linear least squares fitting of XANES spectra corresponding to the S species identified by LCF was applied to the smoothed ME maps to generate maps of individual S species. Speciation map fitting was confirmed by finding the experimental XANES spectra that are the most dissimilar to one another (by PCA on all experimental micro-XANES spectra) and using these as the end-members in the least squares XANES spectra fitting. The former method was chosen to be presented here, due to all experimental XANES spectra containing mixtures of S species. One-way ANOVA was used to determine significant differences to $\alpha = 0.05$ between relative proportions of S species in leaves defined as either uncolonized (<0.002% colonization (n = 7)) or colonized (>1% colonization (n = 11)), and in individual hyaline cells identified as either uncolonized or colonized by epifluorescence. Uncolonized leaf clusters included both negative controls (*Sphagnum* that was not exposed to *Nostoc*) and *Sphagnum* leaves that were inoculated with *Nostoc* but had negligible colonization. No leaves had between 0.002 and 1% colonization.

Results

S speciation in bulk leaf tissue

Sulfur in *Sphagnum* leaves, colonized and uncolonized, consisted primarily of reduced S (13 to 62% of total S), sulfonate (5.4 to 33%), and sulfate (15 to 64%) groups, with lesser overall contributions from elemental S (<21%) and sulfoxides (<10%) (Figure 1; Table 1). Integrated across the entire leaf cluster, which included branch and stem tissue, colonized leaf clusters contained higher relative proportions of sulfate (39 ± 13% versus 22 ± 8%; p = 0.009) and less reduced organic S (26 ± 8% versus 39 ± 11%; p = 0.009) than uncolonized leaf clusters (Figure 2a). The proportion of S present as sulfonate was not significantly different between the two groups. We also observed that the signal to noise ratios in the XANES spectra increased with increasing colonization (Figure 1). The noise of the photon-counting detector follows Poisson counting statistics and is equal to the square root of the number of counts; therefore, higher signal to noise ratios indicate more total S. Higher total S coupled with increasing relative abundance of sulfate indicates that colonized leaves contained more sulfate compounds than uncolonized leaves.

Spatial distribution of S species in uncolonized leaves

The highest abundance of S in uncolonized leaf clusters was observed in the stem tissue (Figure 3; Figure S1). Reduced S and sulfonate were elevated along the stem and in patches on the leaves. Sulfate was low by comparison and relatively evenly distributed, although with slight enrichment in the stem. Isolated leaves with no stems were investigated to better evaluate S distribution in the leaf tissue (Figure 4). Here, the chlorophyllous cells form the internal leaf structure, with higher S associated with the living chlorophyllous cells that surrounded the S-poor hyaline cells. Reduced S was high relative to sulfonate and sulfate, and fairly evenly distributed throughout the leaf, although a few hot spots were observed. Sulfonate and sulfate showed similar distribution patterns but with lower abundance. S K-edge spectra obtained at different spots representing compositional endmembers showed high total amounts of reduced organic S (spots 1-4), sulfonate (spot 5), or sulfate (spots 6 and 7) relative to other areas of the leaf (Figure 4b-d). Reduced S was the dominant species across the leaf except for a couple small areas (e.g., spots 6 and 7) that contained high proportions of sulfonate and sulfate (Figure 4e).

Spatial distribution of S species in Nostoc colonies

Sulfur speciation maps were obtained from *Nostoc* cyanobacteria colonies grown in culture without *Sphagnum* (Figure 5). Sulfur was enriched in the colonies (spots 1 and 4) relative to the surrounding medium and consisted primarily of reduced S. Sulfonate was much less abundant than either reduced organic S or sulfate but was highest in a diffuse zone around the colonies (spots 2, 3, and 5). The media contained low amounts of S as sulfate (spot 6).

Spatial distribution of S species in colonized leaves

Similar to the uncolonized leaf cluster (Figure 3), S species in the colonized leaf cluster were most enriched in the stem tissue (Figure 6; Figure S1). However, S was overall more abundant in the colonized leaves relative to uncolonized leaves and showed dissimilar distributions amongst S species (Figure S2). Sulfate was highly enriched in the stem but low and evenly distributed in the leaves. Sulfonate and reduced organic S were moderately enriched in the stem but with additional patches of enrichment throughout the leaf tissues.

A leaf with no stem was examined to better visualize S distribution in and around colonized hyaline cells (Figure 7). Sulfur enrichment and speciation were heterogenous and differed between hyaline cells identified as either uncolonized or colonized using epifluorescence (Figure 7; Figure S3). Total S was high along the edge of the leaf where the highest concentrations of colonized cells were observed and in colonized cells in the interior of the leaf (spots 1 to 4). Sulfur was relatively low in chlorophyllous cells that formed the edges of hollow, uncolonized hyaline cells in the leaf interior (spots 5 to 9). Low amounts of reduced organic S and sulfate were distributed evenly across the leaf, and sulfate was slightly enriched along the leaf edge (Figure S3). Similar to observations of S distribution in isolated *Nostoc* colonies (Figure 5), hot spots of reduced S were observed in colonized cells and surrounded by diffuse enrichment of sulfonate. Averaged across the individual spots, colonized cells contained higher proportions of reduced organic S (62 ± 5%) than uncolonized cells (34 ± 7%) ($p < 0.001$) and lower proportions of sulfate (3.9 ± 5.2% versus 33 ± 9%, respectively) ($p < 0.001$) (Figure 2; Table 2). Relative proportions of elemental S (6.3 ± 4.6%), sulfoxide (2.8 ± 3.9%), and sulfonate (24 ± 6%) were similar between the two groups ($p > 0.05$). Note that each spot contains contributions from both the hyaline cell and its surrounding chlorophyllous cells. The S composition of uncolonized leaf cells was comparable to uncolonized leaf clusters (Figure 2), although the proportion of sulfate in uncolonized cells was slightly higher.

Discussion

Sphagnum mosses that were not colonized by *Nostoc* cyanobacteria contained a mixture of reduced organic S and oxidized sulfonate- and sulfate-containing compounds in their leaves and stems. *Nostoc* colonization of *Sphagnum* hyaline cells led to increases in total S and in the proportion of S present as sulfate at the scale of the leaf cluster (leaves + stems), indicating that colonization stimulated uptake and/or production of sulfate-containing compounds by *Sphagnum* (Figure 8). Sulfate enrichment in colonized leaf clusters was most prominent in the stems and in leaf margins. These results are consistent with recent studies indicating that *Sphagnum* interaction with *Nostoc* cyanobacteria results in metabolite exchange, with *Nostoc* exuding

N-rich purines and amino acids while depleting carbohydrates (e.g., trehalose) and oxidized S compounds (e.g., choline-O-sulfate, taurine, and sulfoacetate) provided by *Sphagnum* (Carrell et al., 2022; Nagy et al., 2019; Veličković et al., 2018). That is, higher sulfate in leaf clusters may be explained by increased sulfate uptake from the media and subsequent production of sulfate-containing compounds by *Sphagnum* in response to colonization. Sulfate enrichment occurs largely within the stems, possibly due to enhanced nutrient uptake from solution relative to leaves (Fritz et al., 2014) and storage prior to translocation to leaf tissue (Rydin and Clymo, 1989; Aldous, 2002; Salmon et al., 2021).

At the scale of individual hyaline cells, colonized cells exhibited localized enrichment of reduced S, as represented by the amino acid methionine, surrounded by diffuse sulfonate (Figure 8). These patterns were similar to observations of cyanobacteria colonies cultured in the absence of leaves. Non-occupied hyaline cells and their surrounding chlorophyllous cells in colonized leaves were compositionally similar to bulk uncolonized leaves (Figure 2). Sulfate depletion in individual colonized hyaline cells and coexisting enrichment of reduced S may be explained by microbial conversion of sulfate-containing metabolites to metabolites containing reduced S, e.g., amino acids or the antioxidant methionine. Thus, bulk S speciation at the scale of the colonized leaf cluster is dominated by S compounds acquired or produced by *Sphagnum* while S speciation at the scale of the colonized hyaline cell is dominated by S compounds produced in the *Nostoc* biomass.

Although S XANES cannot be used to identify individual metabolites, our findings support observations of metabolite exchange previously reported for *Sphagnum-Nostoc* symbiosis. Specifically, Carrell et al. (2022) report that *Sphagnum* produced sulfate (choline-O-sulfate) and sulfonate (taurine and sulfoacetate) compounds in response to interaction with *Nostoc*. In turn, *Nostoc* increased production of N-containing purines and amino acids. We observed increases in total S and relative sulfate abundance with colonization, consistent with increased production of choline-O-sulfate. Although the relative abundance of sulfonate did not change with colonization in this study, it is possible given increases in total S that the absolute quantity of sulfonate compounds increased as well. High abundance of reduced S in colonized cells is consistent with microbial production of N-rich, S-bearing amino acids such as methionine and cysteine that are potentially transferred to *Sphagnum*. Given that the relative abundance of reduced S decreased with colonization at the scale of the leaf cluster, it is likely that the quantity of reduced S compounds produced by *Nostoc* was small relative to production of sulfate compounds by *Sphagnum*. Nitrogen transfer from *Nostoc* to *Sphagnum* might also occur through S-free purines (Carrell et al. 2021) that are not detectable by these methods.

Sphagnum mosses evaluated here were composed of nearly equal proportions of reduced S (51% ± 12% std.dev.) and oxidized S (49% ± 12% std.dev.) averaged across all bulk leaf clusters, although the relative proportion of these groups varied with colonization by cyanobacteria as discussed above. Our results are consistent with Pierce et al. (2022), who reported relative abundance of 43-46% oxidized S (largely sulfone and sulfonate) and 46-51% reduced S (as thiol, organic monosulfide, thiophene, and organic disulfide) in bulk tissue of representative *Sphagnum* species obtained from the Marcell Experimental Forest in northern Minnesota. Peat soil derived in part from decomposed *Sphagnum* was composed almost entirely of organic S with increasing proportions of reduced S compounds with depth. Pierce et al. (2022) and others (Prietzel et al., 2009a; Prietzel et al., 2009b) have shown that S speciation in wetland soils is highly dependent on saturation. Sulfur in persistently saturated and anoxic soils accumulates primarily as reduced organic S (e.g., thiols, organic monosulfides) (Prietzel et al., 2009a; Pierce et al., 2022) and/or as iron sulfide minerals where Fe is abundant (Prietzel et al., 2009b), while periodic oxygenation results in higher proportions of moderately to highly oxidized S species. In contrast to *Sphagnum* decomposition, leaf litter decomposition in a northern hardwood forest resulted in rapid decreases in reduced S and relative increases in sulfonate and sulfate (Schroth et al., 2007). These differences in S compounds in decomposed organic matter likely result from contrasting redox conditions, where the peat decomposes under increasingly anoxic conditions with depth while the forest litter undergoes oxidative decomposition. Our study indicates that mutualistic interactions with cyanobacteria may result in at least temporary increases in oxidized S compounds within *Sphagnum* tissues that subsequently undergo anaerobic decomposition in saturated peat soils. The net increase in oxidized S and its potential to support anaerobic sulfate reduction by peat microorganisms remain unclear.

This study provides novel evidence for the change in S speciation that occurs in *Sphagnum* mosses that develop mutualistic interactions with *Nostoc* cyanobacteria. Overall, our observations emphasize the potential importance of S metabolite production by *Sphagnum* for facilitating symbiotic association with N_2-fixers. Additional studies are needed to determine the role of S exchange in driving ecosystem-scale S, N, and C dynamics. For example, this study did not quantify rates of uptake or increases in total S that occurred following *Nostoc* colonization of *Sphagnum*, or evaluate how S availability affected colonization or N_2-fixation rates. It also remains unknown how this metabolite exchange is sensitive to environmental conditions, or what role it might play in enabling *Sphagnum* to persist in warming climates. Future studies to address these uncertainties could enable better understanding of how Sphagnum-driven S dynamics influence associated C and N inputs to peatland ecosystems.

Data availability

All sulfur K-edge XANES spectra and μ-XRF maps are available in the Stanford Digital Repository at https://doi.org/10.25740/wx458ym7322.

Acknowledgements

Use of the Stanford Synchrotron Radiation Lightsource (SSRL), SLAC National Accelerator Laboratory, is supported by the DOE, Office of Science, Office of Basic Energy Sciences under contract DE-AC02-76SF00515. The SSRL Structural Molecular Biology Program is supported by the DOE-BER, and by the National Institutes of Health (NIH), National Institute of General Medical Sciences (NIGMS; P30GM133894). The contents of this publication are solely the responsibility of the authors and do not necessarily represent the official views of the NIGMS or the NIH. J.R is supported by supplemental funding from DOE-BER to assist and expand biological and environmental relevant research and users at SSRL. Collection of starting *Sphagnum angustifolium* was made possible through the SPRUCE project, which is supported by Office of Science; Biological and Environmental Research (BER); US Department of Energy (DOE), Grant/Award Number: DE-AC05–00OR22725. Experimentation and some analyses were supported by the DOE BER Early Career Research Program. This work was also supported by the ORNL Critical Interfaces Science Focus Area sponsored by the DOE Office of Science Biological and Environmental Research Program. Oak Ridge National Laboratory is managed by UT-Battelle, LLC, for the US DOE under contract no DE-AC05–00OR22725.

Author contributions

Elizabeth Herndon: conceptualization, formal analysis, writing, project administration; Jocelyn Richardson: conceptualization, methodology, formal analysis, writing; Alyssa Carrell: methodology, formal analysis, writing; Eric Pierce: conceptualization, funding acquisition; David Weston: conceptualization, writing, funding acquisition.

Competing interests

None declared.

References:

Aldous AR. 2002. Nitrogen retention by Sphagnum mosses: responses to atmospheric nitrogen deposition and drought. *Canadian Journal of Botany*, **80**(7): 721-731.

Basilier K (1979) Moss-Associated Nitrogen-Fixation in Some Mire and Coniferous Forest Environments around Uppsala, Sweden. Lindbergia 5, 84-88.

Basilier K, Granhall U, & Stenström TA. 1978. Nitrogen fixation in wet minerotrophic moss communities of a subarctic mire. Oikos, 236-246

Belyea LR, and Malmer N. 2004. Carbon sequestration in peatland: patterns and mechanisms of response to climate change. *Global Change Biology*, **10**(7), pp.1043-1052.

Berg A, Danielsson Å, Svensson BH. 2013. Transfer of fixed-N from N 2-fixing cyanobacteria associated with the moss Sphagnum riparium results in enhanced growth of the moss. Plant and soil. **362**:271-8.

Carrell AA, Kolton M, Glass JB, Pelletier DA, Warren MJ, Kostka JE, Iversen CM, Hanson PJ, Weston DJ. 2019. Experimental warming alters the community composition, diversity, and N2 fixation activity of peat moss (Sphagnum fallax) microbiomes. Global Change Biology **25**: 2993–3004

Carrell AA, Veličković D, Lawrence TJ, Bowen BP, Louie KB, Carper DL, Chu RK, Mitchell HD, Orr G, Markillie LM, et al. 2021. Novel metabolic interactions and environmental conditions mediate the boreal peatmoss-cyanobacteria mutualism. The ISME Journal **16**: 1074–1085.

Carrell AA, Lawrence TJ, Grace K, Cabugao M, Carper DL, Pelletier DA, Lee JH, Jawdy SS, Grimwood J, Schmutz J, et al. 2022. Habitat-adapted microbial communities mediate Sphagnum peatmoss resilience to warming. New Phytologist **234**: 2111–2125.

Clymo RS, Hayward PM. 1982. The ecology of Sphagnum. In: Smith AJE, ed. Bryophyte ecology. Dordrecht, the Netherlands: Springer, 229–289.

Dorrepaal E, Toet S, Van Logtestijn RSP, Swart E, Van De Weg MJ, Callaghan T V., Aerts R. 2009. Carbon respiration from subsurface peat accelerated by climate warming in the subarctic. Nature **460**: 616–619.

Fritz C, Lamers LP, Riaz M, van den Berg LJ and Elzenga TJ. 2014. Sphagnum mosses-masters of efficient N-uptake while avoiding intoxication. *PloS one*, **9**(1), p.e79991.

Granhall U, Hofsten AV. 1976. Nitrogenase Activity in Relation to Intracellular Organisms in Sphagnum Mosses. Physiologia Plantarum **36**, 88-94.

Hanson PJ, Griffiths NA, Iversen CM, Norby RJ, Sebestyen SD, Phillips JR, Chanton JP, Kolka RK, Malhotra A, Oleheiser KC, Warren JM. Rapid net carbon loss from a whole-ecosystem warmed peatland. AGU Advances. 2020 Sep;1(3):e2020AV000163.

Janssen KA, Vitosh ML. 1974. Effect of Lime, Sulfur, and Molybdenum on N_2 Fixation and Yield of Dark Red Kidney Beans 1. Agronomy Journal. **66**(6):736-40.

Kip N, van Winden JF, Pan Y, et al. 2010. Global prevalence of methane oxidation by symbiotic bacteria in peat-moss ecosystems. Nature Geoscience **3**, 617-621

Kostka JE, Weston DJ, Glass JB, Lilleskov EA, Shaw AJ, Turetsky MR. 2016. The Sphagnum microbiome: new insights from an ancient plant lineage. New Phytologist **211**:57–64.

Limpens J, Heijmans, MM, and Berendse, F. 2006. The nitrogen cycle in boreal peatlands. In *Boreal peatland ecosystems* (pp. 195-230). Berlin, Heidelberg: Springer Berlin Heidelberg.

Lin X, Tfaily MM, Steinweg JM, Chanton P, Esson K, Yang ZK, Chanton JP, Cooper W, Schadt CW, and Kostka JE. 2014. Microbial community stratification linked to utilization of carbohydrates and phosphorus limitation in a boreal peatland at Marcell Experimental Forest, Minnesota, USA. *Applied and environmental microbiology*, **80**(11), pp.3518-3530.

Lindo Z, Nilsson MC, and Gundale MJ. 2013. Bryophyte-cyanobacteria associations as regulators of the northern latitude carbon balance in response to global change. Global Change Biology, **19**(7): p. 2022-2035.

Manceau A, Nagy KL. 2012. Quantitative analysis of sulfur functional groups in natural organic matter by XANES spectroscopy. Geochimica et Cosmochimica Acta, **99**, 206–223. https://doi.org/10.1016/j.gca.2012.09.033

Newville M. 2013. Larch: An Analysis Package for XAFS and Related Spectroscopies. Journal of Physics: Conference Series, **430**, 012007. https://doi.org/10.1088/1742-6596/430/1/012007

Norby RJ, Childs J, Hanson PJ, Warren JM. 2019. Rapid loss of an ecosystem engineer: Sphagnum decline in an experimentally warmed bog. *Ecology and Evolution* **9**: 12571–12585.

Petro C, Carrell AA, Wilson RM, Duchesneau K, Noble-Kuchera S, Song T, Iversen CM, Childs J, Schwaner G, Chanton JP, Norby RJ, Hanson PJ, Glass JB, Weston DJ, Kostka JE. Climate drivers alter nitrogen availability in surface peat and decouple N2 fixation from CH4 oxidation in the Sphagnum moss microbiome. 2023. Global Change Biology, https://doi.org/10.1111/gcb.16651

van der Ploeg JR, Eichhorn E, Leisinger T. 2021. Sulfonate-sulfur metabolism and its regulation in Escherichia coli. Arch Microbiol. **176**: 1–8

Pierce CE, Furman OS, Nicholas SL, Wasik JC, Gionfriddo CM, Wymore AM, Sebestyen SD, Kolka RK, Mitchell CP, Griffiths NA, Elias DA, Nater EA, and Toner BM. 2022. Role of ester sulfate and organic disulfide in mercury methylation in peatland soils. *Environmental science & technology*, **56**(2), pp.1433-1444.

Prietzel J, Thieme J, Tyufekchieva N, Paterson D, McNulty I, and Kögel-Knabner I., 2009. Sulfur speciation in well-aerated and wetland soils in a forested catchment assessed by sulfur K-edge X-ray absorption near-edge spectroscopy (XANES). *Journal of Plant Nutrition and Soil Science*, **172**(3), pp.393-403.

Prietzel J, Tyufekchieva N, Eusterhues K, Kögel-Knabner I, Thieme J, Paterson D, McNulty I, de Jonge M, Eichert D, and Salomé M. 2009. Anoxic versus oxic sample pretreatment: Effects on the speciation of sulfur and iron in well-aerated and wetland soils as assessed by X-ray absorption near-edge spectroscopy (XANES). *Geoderma*, **153**(3-4), pp.318-330.

Rydin H. and Clymo RS. 1989. Transport of carbon and phosphorus compounds about Sphagnum. *Proceedings of the Royal Society of London. B. Biological Sciences*, **237**(1286), pp.63-84.

Salmon VG, Brice DJ, Bridgham S, Childs J, Graham J, Griffiths NA, Hofmockel K, Iversen CM, Jicha TM, Kolka RK, and Kostka JE. 2021. Nitrogen and phosphorus cycling in an ombrotrophic peatland: a benchmark for assessing change. *Plant and Soil*, **466**, 649-674.

Shock CC, Williams WA, Jones MB, Center DM, Phillips DA 1984. Nitrogen fixation by subclover associations fertilized with sulfur. *Plant and Soil* **81**:323-32.

Scherer HW, Lange A. 1996. N_2 fixation and growth of legumes as affected by sulphur fertilization. *Biology and Fertility of Soils*. **23**: 449-53.

Scherer HW, Pacyna S, Manthey N, Schulz M. 2006. Sulphur supply to peas (Pisum sativum L.) influences symbiotic N_2 fixation. *Plant, Soil and Environment*. **52**(2):72-7.

Stuart RK, Pederson ER, Weyman PD, Weber PK, Rassmussen U, Dupont CL. 2020. Bidirectional C and N transfer and a potential role for sulfur in an epiphytic diazotrophic mutualism. *ISME Journal* **14**: 3068–3078.

Urban NR, and Eisenreich SJ. 1988. Nitrogen cycling in a forested Minnesota bog. *Canadian Journal of Botany*, **66**(3), pp.435-449.

Urban NR, Eisenreich SJ, and Grigal DF. 1989. Sulfur cycling in a forested Sphagnum bog in northern Minnesota. *Biogeochemistry*, **7**, pp.81-109.

Varin S, Cliquet JB, Personeni E, Avice JC, Lemauviel-Lavenant S. 2010. How does sulphur availability modify N acquisition of white clover (Trifolium repens L.)? *Journal of Experimental Botany* **61**(1):225-34.

Vile MA, Bridgham SD, Wieder RK, and Novák M. 2003. Atmospheric sulfur deposition alters pathways of gaseous carbon production in peatlands. *Global Biogeochemical Cycles*, **17**(2).

Warshan D, Espinoza JL, Stuart RK, Richter RA, Kim S-Y, Shapiro N, et al. 2017. Feathermoss and epiphytic Nostoc cooperate differently: expanding the spectrum of plant–cyanobacteria symbiosis. *ISME J.* **12**:1–13.

Webb SM. 2005. SIXPack a Graphical User Interface for XAS Analysis Using IFEFFIT. *Physica Scripta* (T115), 1011. https://doi.org/10.1238/Physica.Topical.115a01011

Webb SM. 2006. SMAK: Sam's Microprobe Analysis Kit, V 0.46; Stanford Synchrotron Radiation Laboratory: Stanford, CA

Weston DJ, Timm CM, Walker AP, Gu L, Muchero W, Schmutz J, Shaw AJ, Tuskan GA, Warren JM, Wullschleger SD. 2015. Sphagnum physiology in the context of changing climate: Emergent influences of genomics, modelling and host–microbiome interactions on understanding ecosystem function. *Plant, cell & environment.* **38**(9):1737-51.

Wilson RM, Hopple AM, Tfaily MM, Sebestyen SD, Schadt CW, Pfeifer-Meister L, Medvedeff C, Mcfarlane KJ, Kostka JE, Kolton M, et al. 2016. Stability of peatland carbon to rising temperatures. Nature Communications **7**: 1–10

Yin T, Feng M, Qiu C, and Peng S. 2022. Biological nitrogen fixation and nitrogen accumulation in peatlands. *Frontiers in Earth Science*, **10**: p.670867.

Yu Z, Campbell ID, Campbell C, Vitt DH, Bond GC, and Apps MJ. 2003. Carbon sequestration in western Canadian peat highly sensitive to Holocene wet-dry climate cycles at millennial timescales. *The Holocene*, **13**(6), pp.801-808.

Yu ZC. 2012. Northern peatland carbon stocks and dynamics: A review. *Biogeosciences* **9**: 4071–4085.

Figure Captions

Figure 1. (left) Sulfur K-edge XANES spectra obtained on *Sphagnum angustifolium* leaf tissue using an unfocused beam, arranged from uncolonized leaves on bottom to leaves most highly colonized by *Nostoc muscorum* at the top. Line colors for each spectrum correspond to a binned colonization percentage: <1% (grey), 1-5% (golden), 5-10% (green), and > 10% (purple). Vertical dashed lines indicate the peak position of the indicated S functional group. Note the increasing signal:noise ratio, indicative of higher S content, with increasing colonization. (right) Relative proportions of S-bearing functional groups obtained from linear combination fits to the corresponding spectra, with the percent colonization of each leaf sample provided to the right of each bar.

Figure 2. Relative proportions of S functional groups in whole leaf clusters of *S. angustifolium* (a) and in individual hyaline cells within a leaf colonized by *N. muscorum* (b), as obtained from linear combination fits. Asterisks indicate significant differences in the proportion of a given S functional group between colonized and uncolonized groups to $p < 0.01$ (**) or $p < 0.001$ (***) as determined using one-way ANOVA. Whole leaves were defined as colonized if percent colonization was >1% (n = 11) and uncolonized if percent colonization was ≤ 0.002% (n = 7). No leaf clusters showed colonization between 0.002% and 1%. Individual cells were defined as colonized (n = 4) or uncolonized (n = 5) based on the presence or absence of cyanobacteria within that cell. Box-and-whisker plots represent the 25-75% (box) and standard deviation (whiskers) of each group, with the mean value shown as an open square and individual values shown as open diamonds.

Figure 3. Sulfur K-edge XANES collected from uncolonized *Sphagnum angustifolium* plant tissue using an unfocused beam (left panel) and corresponding S microprobe maps for reduced S, sulfonate, and sulfate functional groups in a cluster of leaves with attached stem. The scale bar is in micron units, and the color scale represents fluorescent intensity which is proportional to S concentration.

Figure 4. Sulfur K-edge XANES collected from a single uncolonized *Sphagnum angustifolium* leaf using a focused beam (a), and corresponding S microprobe maps for (b) reduced S, (c) sulfonate, and (d) sulfate functional groups. Linear combination fits to each spectrum are shown in panel (e). The scale bar is in micron units, and the color scale represents fluorescent intensity which is proportional to S concentration. Numbers in panel (a) refer to the point location from which the spectrum was collected, indicated in panels (b) to (d).

Figure 5. Sulfur K-edge μXANES collected from points in and around a *Nostoc muscorum* cyanobacterial colony (a), and corresponding S x-ray microprobe maps for (b) total S, (c) reduced S, (d) sulfonate, and (e) sulfate functional groups. Spectra in panel (a) are color coded by whether they were collected from the colony (yellow), the halo around the colony (green), or the surrounding media (blue), and numbers refer to the point location from which the spectrum was collected, indicated in panel (b).The scale bar is in micron units, and the color scale represents fluorescent intensity which is proportional to S concentration.

Figure 6. Sulfur K-edge XANES collected from clusters of *Sphagnum angustifolium* leaves colonized by *Nostoc muscorum* using an unfocused beam (a), and corresponding S microprobe maps for (b) reduced S, (c) sulfonate, and (d) sulfate functional groups for the leaf cluster with 16.2% colonization. Panel (a) includes two spectra from leaf clusters with either 16.2% or 18.6% colonization, as indicated. For panels (b-d), the scale bars are in micron units, and the color scale represents fluorescent intensity which is proportional to S concentration.

Figure 7. A tricolor map of S speciation across a single colonized *Sphagnum angustifolium* leaf (a) with the corresponding epifluorescence image showing *Sphagnum* cells in gold and colonizing *Nostoc*

muscorum in pink (b). The epifluorescence image has been rotated to match the orientation of the leaf in the tricolor map. Sulfur K-edge μXANES for the point locations indicated in the maps are shown in panel (c) with results of linear combination fits to each μXANES spot shown in panel (d). The color scale in panel (a) represents fluorescent intensity, which is proportional to concentration, for the three indicated S species. In panel (c), spectra from colonized hyaline cells identified with epifluorescence are shown in pink (1 - 4) and uncolonized cells are shown in gold (5 - 9).

Figure 8. Conceptual diagram of S speciation in stem and leaf tissue of *Sphagnum angustifolium* moss with hyaline cells that are either uncolonized or colonized by *Nostoc muscorum* cyanobacteria. Uncolonized hyaline cells were found both in *Sphagnum* that was exposed to *Nostoc* but did not colonize and in negative controls where *Sphagnum* was not exposed to *Nostoc*. While uncolonized stems and leaves contain relatively low S present primarily as reduced S, colonized tissues exhibit S enrichment (as sulfate) in stems and leaf edges and in hot spots of reduced S localized to colonized hyaline cells.

Table 1. Relative proportions of individual S species determined using Linear Combination Fits to bulk XANES spectra from whole *Sphagnum angustifolium* leaf clusters, organized by colonization by *Nostoc muscorum* (%) determined using epifluorescence. Relative contributions of each spectrum have been normalized to 100%.

Colonization (%)	S°	Reduced S	Sulfoxide	Sulfonate	Sulfate	R-factor
0	10.4	31.0	7.3	16.5	34.7	0.004
0	13.5	35.1	9.5	19.2	22.8	0.020
0	11.2	45.4	7.9	19.4	16.1	0.003
0	5.4	28.3	2.6	33.5	30.2	0.005
0.001	13.7	35.9	9.1	25.4	15.8	0.007
0.001	12.0	38.2	7.0	24.1	18.7	0.002
0.002	6.7	62.3	0.0	16.0	15.0	0.020
1.1	12.9	23.6	8.1	26.7	28.7	0.006
1.4	20.7	18.4	7.4	12.7	40.8	0.011
1.8	10.9	22.5	7.3	28.4	30.8	0.006
1.9	11.7	13.4	6.7	25.2	42.9	0.006
3.8	12.0	33.3	8.5	9.0	37.1	0.004
6.8	12.1	18.7	6.6	12.4	50.2	0.010
7.2	5.2	19.2	6.4	5.4	63.8	0.005
9.3	14.7	34.8	9.4	18.0	23.0	0.010
10.8	14.8	40.0	8.8	20.2	16.1	0.003
16.2	9.3	25.5	8.2	10.6	46.3	0.006
18.6	8.9	32.0	4.8	8.9	45.5	0.008

559 **Table 2**. Relative proportions of individual S species present in cells within *Sphagnum angustifolium*
560 leaves that are either uncolonized or colonized by *Nostoc muscorum*, as determined using Linear
561 Combination Fits to μXANES spectra from individual spots in Figure 7. Relative contributions of each
562 spectrum have been normalized to 100%.

Spot No.	Colonized	S° (%)	Reduced S (%)	Sulfoxide (%)	Sulfonate (%)	Sulfate (%)	R-factor
1	yes	11.4	58.4	0.0	25.5	4.8	0.019
2	yes	0.0	58.5	6.9	23.6	11.0	0.008
3	yes	13.3	63.8	0.0	23.0	0.0	0.008
4	yes	9.8	68.0	0.0	22.2	0.0	0.014
5	no	5.5	29.4	4.0	24.5	36.7	0.013
6	no	4.5	24.9	0.0	36.5	34.1	0.012
7	no	5.8	44.5	0.0	24.5	25.3	0.012
8	no	6.9	36.5	10.6	22.3	23.7	0.005
9	no	0.0	36.0	4.1	14.6	45.3	0.008

563

564

565

566 **Figure 1.**

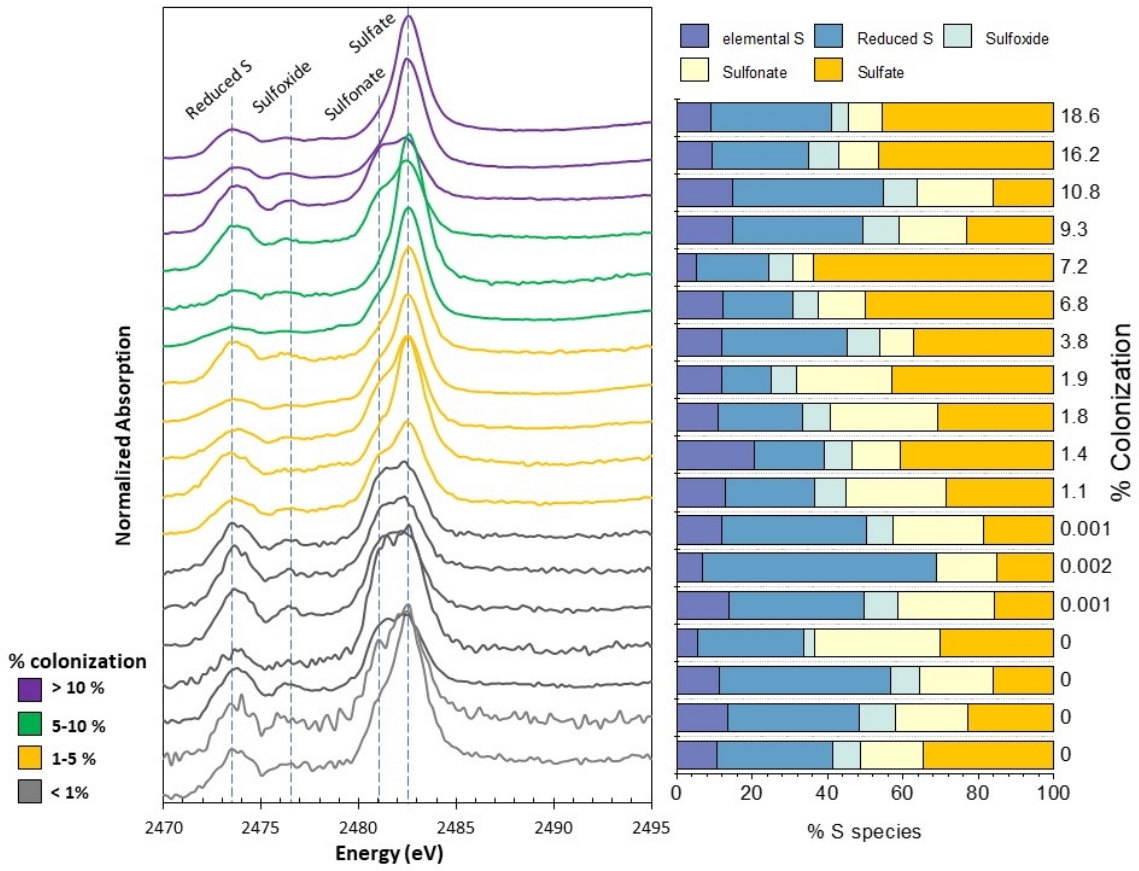

567

568

569 **Figure 2.**

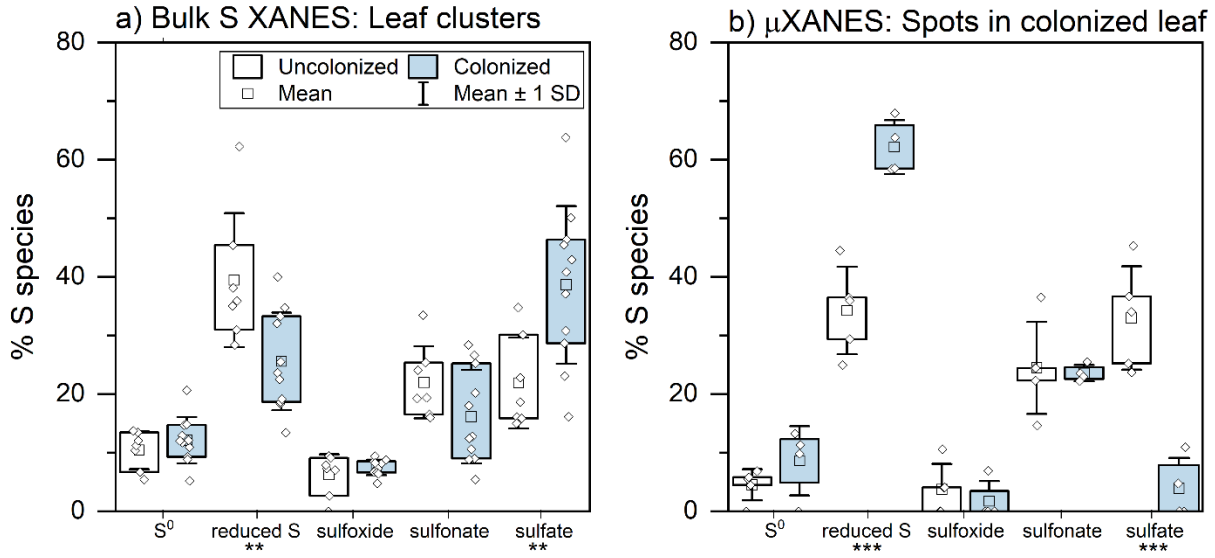

570

571

572 **Figure 3.**

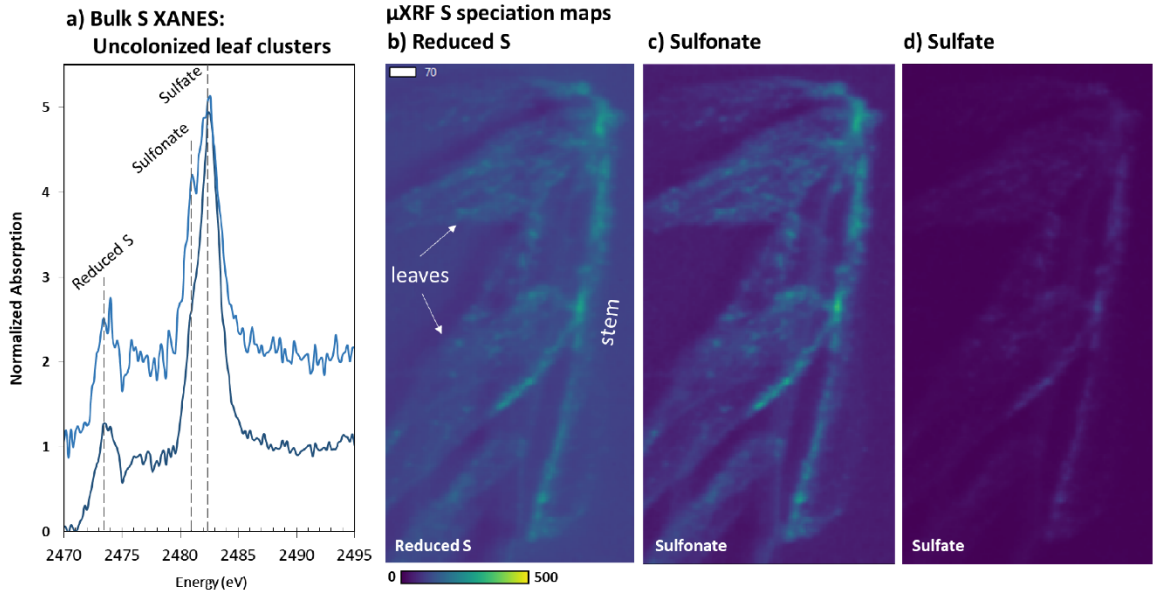

573

574

575 **Figure 4.**

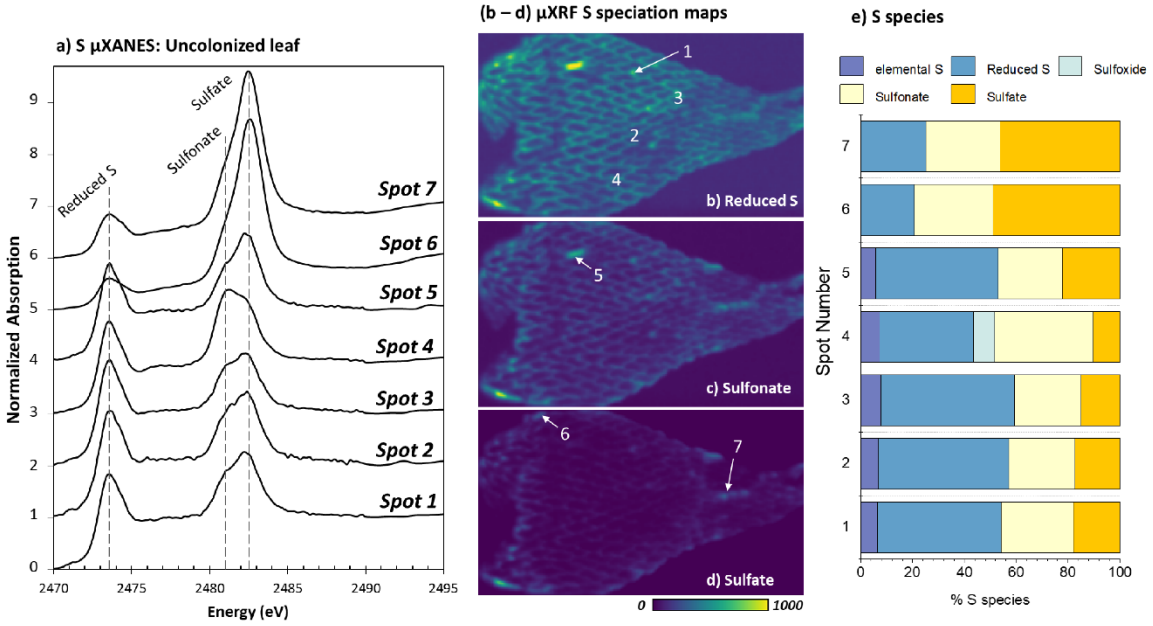

576

577

578 **Figure 5.**

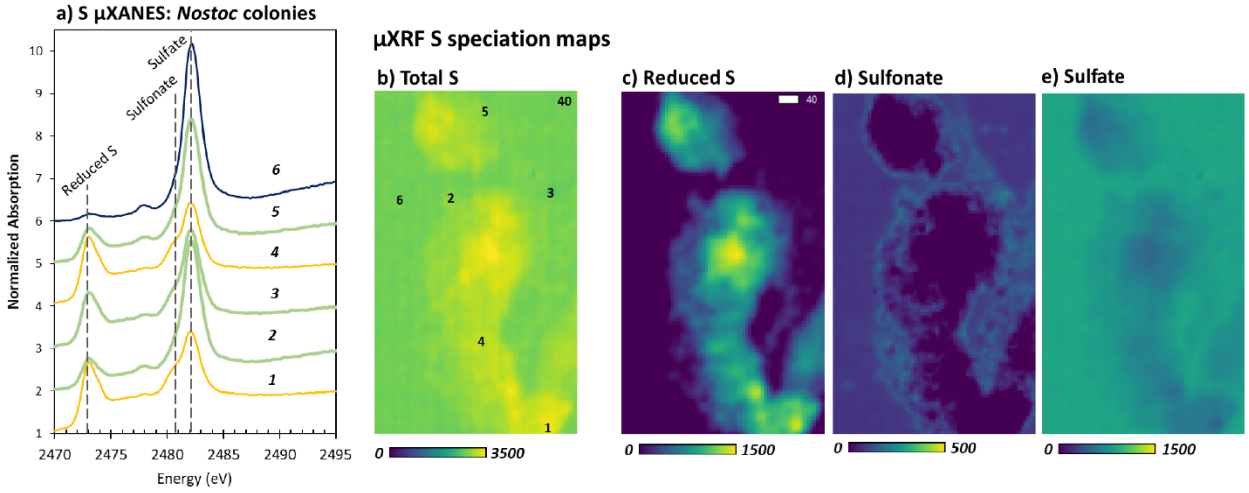

579

580

581 **Figure 6.**

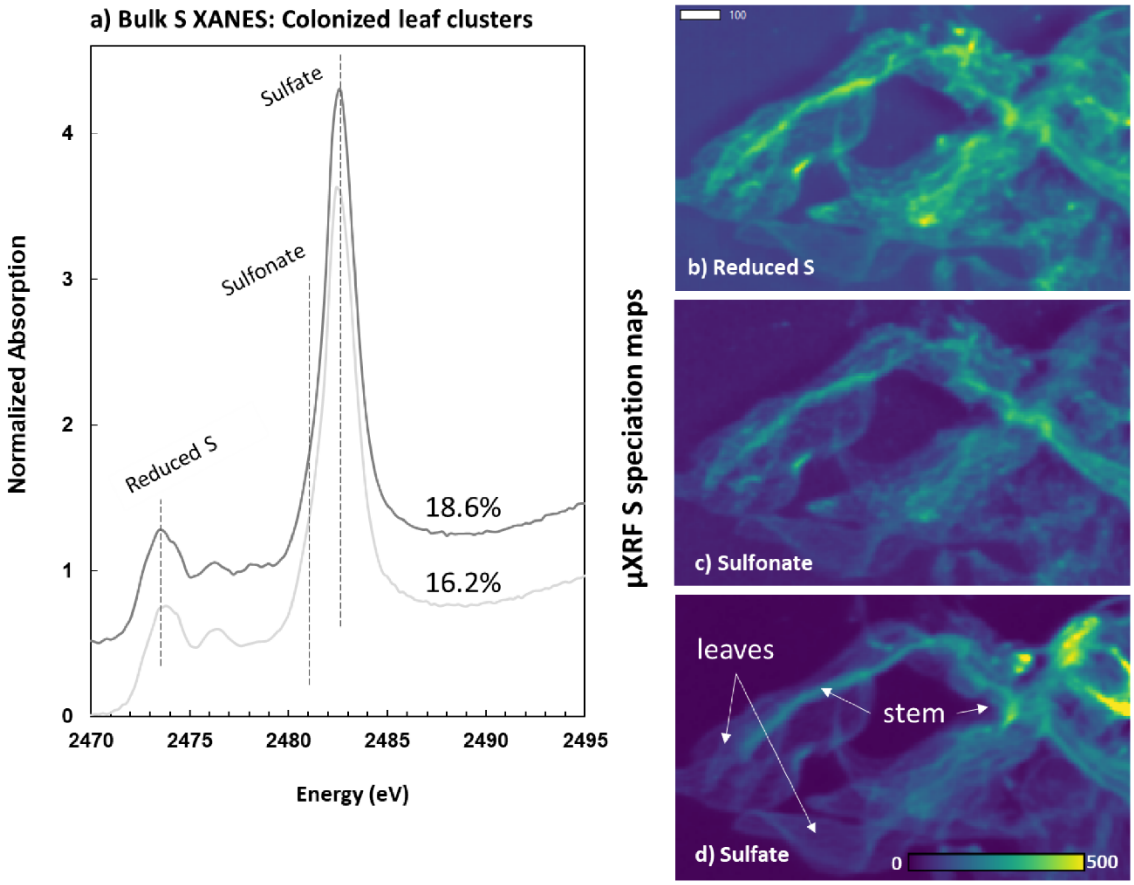

582

583

584 **Figure 7.**

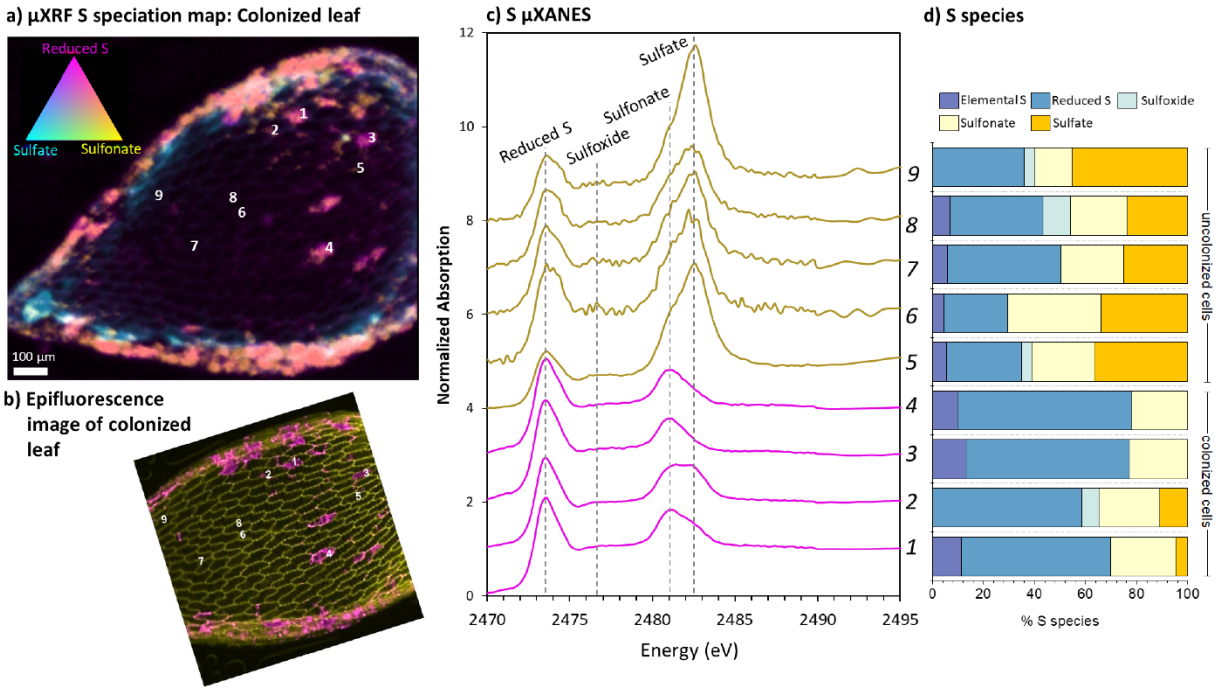

585

586

587

588 **Figure 8.**

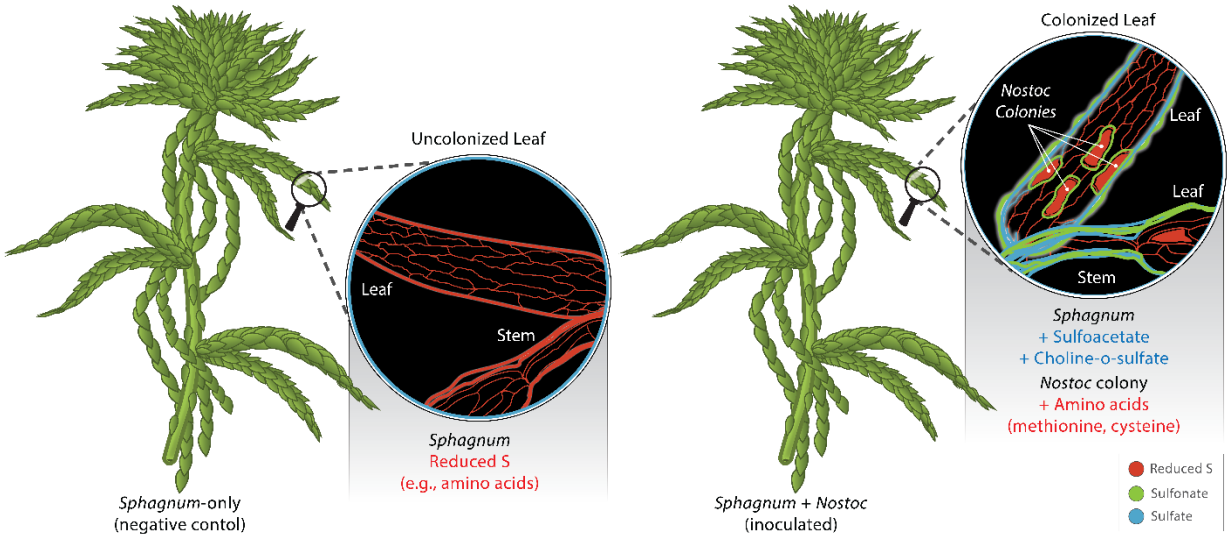

589

590

Supporting Information

The supporting information contains three additional figures.

Figure S1. Micro-XRF maps of total S in colonized and uncolonized individual leaves and leaf clusters.

Figure S2. Micro-XRF maps of S species in uncolonized and colonized individual leaves.

Figure S3. Micro-XRF maps of total S and S species in sections of a colonized leaf.